To *Journal of Human Genetics*

Title page

Title:

Effect of *CYP3A5*3* genetic variant on the metabolism of direct-acting antivirals *in vitro*: a different effect on asunaprevir versus daclatasvir and beclabuvir

Author names and affiliations:

Jun Matsumoto[1,*], Su Nwe San[2], Masachika Fujiyoshi[1], Ayano Kawauchi[2], Natsumi Chiba[2], Ran Tagai[2], Ryoko Sanbe[2], Shiho Yanaka[2], Hiroaki Sakaue[3], Yoshinori Kato[2], Hiroyoshi Nakamura[2,4], Harumi Yamada[2], and Noritaka Ariyoshi[1]

[1]Department of Personalized Medicine and Preventive Healthcare Sciences, Graduate School of Medicine, Dentistry and Pharmaceutical Sciences, Okayama University, Okayama, Japan

[2]Department of Pharmacokinetics, Pharmaceutical Sciences, International University of Health and Welfare, Tochigi, Japan

[3]Department of Biochemistry, School of Pharmacy, Tokyo University of Pharmacy and Life Sciences, Tokyo, Japan

[4]Division of Pharmacy, International University of Health and Welfare Mita Hospital,

Tokyo, Japan

*Corresponding author

Corresponding author:

Jun Matsumoto, Ph.D.

Address: 2-5-1 Shikata-cho, Kita-ku, Okayama, 700-8558, Japan

Email address: matsumotoj@okayama-u.ac.jp

Number of figures: 3

Number of tables: 3

Number of supplementary figures: 4

Number of supplementary tables: 3

Number of words in the Abstract: 193/200

Number of words: 4553/5000

Conflict of Interest: The authors declare that they have no conflict of interest.

Abstract

Direct-acting antivirals, asunaprevir (ASV), daclatasvir (DCV), and beclabuvir (BCV) are known to be mainly metabolized by CYP3A enzymes; however, the differences in the detailed metabolic activities of CYP3A4 and CYP3A5 on these drugs are not well clarified. The aim of the present study was to elucidate the relative contributions of CYP3A4 and CYP3A5 to the metabolism of ASV, DCV, and BCV as well as the effect of *CYP3A5*3* genetic variant *in vitro*. The amount of each drug and their major metabolites were determined using LC-MS/MS. Recombinant CYP3As and *CYP3A5*3*-genotyped human liver microsomes (CYP3A5 expressers or non-expressers) were used for the determination of their metabolic activities. The contribution of CYP3A5 to ASV metabolism was considerable compared to that of CYP3A4. Consistently, ASV metabolic activity in CYP3A5 expressers was higher than those in CYP3A5 non-expresser. Moreover, CYP3A5 expression level was significantly correlated with ASV metabolism. In contrast, these observations were not found in DCV and BCV metabolism. To our knowledge, this is the first study to directly demonstrate the effect of *CYP3A5*3* genetic variants on the metabolism of ASV. The findings of the present study may provide basic information on ASV, DCV, and BCV metabolisms.

Introduction

Hepatitis C is a hepatic disease caused by the hepatitis C virus (HCV) infection. There are at least seven different HCV genotypes (GT) (ref. 1). The global distribution of the HCV GTs is complex. In general, GT1, 2, 3, and 4 are widely distributed across geographic areas and GT 5, 6, and 7 are the most restricted (ref. 1, 2). GT1 is commonly observed in many areas including Asia, Europe, South and North America, and Australia, while GT2 is more restricted and frequently found in West Africa and parts of South America. GT3 is typically dominant in South Asia and GT4 is frequently found from central Africa to the Middle East. GT1 is the most prevalent HCV GT worldwide at 46%, followed by GT3 (22%), GT2 (13%), and GT4 (13%) (ref. 2). Interferon (IFN)-based therapy in combination with ribavirin, aiming at stimulating patient's immune system to eliminate HCV virus, was once the standard treatment against HCV GT1 infection worldwide. However, the incidence of significant adverse effects (AEs) including interstitial pneumonia, depression, suicide ideation, and thrombocytopenia caused by IFN was relatively high, and the rate of sustained virological responses (SVR), which is defined as undetectable HCV RNA expressions in the blood after certain period of treatment duration, was unsatisfied. In recent years, several direct-acting antivirals (DAAs) have been developed (ref. 3). DAAs have higher SVR

rate, weaker AEs, and shorter treatment durations than IFN-based therapy (ref. 4). The IFN-based therapy has been therefore replaced by DAAs.

Asunaprevir (ASV) and daclatasvir (DCV) (Figures 1A and 1B) are the first developed DAAs, and they were approved as the first oral DAA combination therapy against HCV GT1 globally. These two DAAs have different targeted-sites on HCV. ASV and DCV act as a nonstructural protein 3 protease inhibitor and as a 5A replication complex inhibitor, respectively (ref. 5, 6). ASV/DCV combination therapy has significantly contributed to the improved SVR rate in HCV GT1 infection (ref. 7). However, it has been known that mutated-HCV exhibits resistance to ASV and DCV (ref. 8, 9). Beclabuvir (BCV, Figure 1C) is a nonstructural protein 5B replication complex inhibitor (ref. 10). BCV showed additive synergistic effects on replicon inhibition to particularly the resistant HCV in combination with ASV/DCV (ref. 10–12). SVR rate was further improved using a combination tablet composed of ASV/DCV/BCV (ref. 13), although the risk of several AEs such as liver injury still remains.

The cytochrome P450 (CYP) 3A family of enzymes is important in the metabolism of numerous clinically used drugs including several DAAs. Four CYP3A isoforms have been reported in humans: CYP3A4, CYP3A5, CYP3A7, and CYP3A43

(ref. 14). Because CYP3A7 is a predominant enzyme in fetal liver and CYP3A43 is expressed at low levels, CYP3A4 and CYP3A5 are the two major CYP3A enzymes responsible for drug metabolism in adult human liver (ref. 14, 15). Recent studies have shown that CYP3A4 and CYP3A5 exhibit some differences in substrate specificity (ref. 16, 17). For example, the immunosuppressive drug tacrolimus is predominantly metabolized by CYP3A5. Therefore, the expression level of CYP3A5 affects the metabolic rate of this drug more significantly than the expression level of CYP3A4 does (ref. 18–20). A recent paper elucidated the X-ray crystal structure of CYP3A5 by using ritonavir (RTV), which is a substrate/strong inhibitor for both CYP3A4 and CYP3A5, and compared the structure of CYP3A5 with that of CYP3A4 (ref. 21). CYP3A4 and CYP3A5 share 84% of their amino acid sequence and the secondary and tertiary structures are very similar; however, the architecture of their active sites is different. This may cause the difference in substrate specificities between CYP3A4 and CYP3A5. Importantly, all the three DAAs; ASV, DCV, and BCV, are considered to be mainly metabolized by CYP3A enzymes (ref. 22–24). However, the differences in the detailed metabolic activities of these three drugs between CYP3A4 and CYP3A5 are ambiguous. The most investigated and common *CYP3A* genetic variant is *CYP3A5*3*, which contributes to substantial inter-individual variation in the protein expression of CYP3A5

(ref. 25). Individual homozygous for *CYP3A5*3* allele either do not express or expresses faint amount of CYP3A5 protein. Thus, *CYP3A5*3* variant may change the metabolism of drugs are predominantly metabolized by CYP3A5 or by both CYP3A4 and CYP3A5.

There are still a few difficult-to-treat patients even with the use of the combination tablet of ASV/DCV/BCV. The AEs, such as alanine aminotransferase (ALT) elevation, occur in approximately 50% of patients, and it is strongly recommended to monitor the liver function of patients while using the ASV/DCV/BCV combination therapy (ref 26). Importantly, there is a need to stop using the tablet of ASV/DCV/BCV when severe AEs are observed. However, the detailed mechanism and the significant mechanistic factors for the interindividual-variation in the incidence of AEs caused by these drugs have not yet been elucidated. If the contributions of CYP3A5 to the metabolism of these drugs are significant, it is likely that CYP3A5 expression defined as information on the *CYP3A5*3* variant may affect the blood concentration of ASV, DCV, and BCV and the incidence of AEs via changing their metabolic ratio.

In this study, the detailed relative contributions of CYP3A4 and CYP3A5 to metabolism of ASV, DCV, and BCV *in vitro* were elucidated in recombinant CYP3As

(rCYP3A). Moreover, the effects of *CYP3A5*3* variant on the metabolism to these three drugs were examined by using human liver microsome (HLM). To our knowledge, this is the first study to suggest directly one of mechanical factors for inter-individual variation of ASV, DCV, and BCV metabolisms.

Materials and methods

Materials

ASV, DCV, BCV, and RTV were purchased from Chem Scene (Monmouth Junction, NJ). Unless otherwise indicated, all chemicals and solvents were of the highest commercial or LC-MS/MS grade and purchased from Wako (Osaka, Japan). rCYP3A4, rCYP3A5 (microsomes from baculovirus-infected insect cells containing human cytochrome P450 reductase and human cytochrome b_5 with cDNA-expressed human CYP3A4 or CYP3A5), and NADPH regenerating solution were purchased from Corning Gentest (Woburn, MA). Control microsomes from baculovirus-infected insect cells containing human cytochrome P450 reductase and human cytochrome b5 without cDNA-expressed human CYP3As (Corning Gentest) were used as a baseline for all experiments. Thirty-nine frozen human liver tissues obtained from Human and Animal Bridging Research Organization (Chiba, Japan) in our previous study were used in the present study (Subject distribution by race and ethnicity: 28 White (72%), 6 Hispanic (15%), 3 African American (8%), and 2 Asian (5%)) (ref. 27). The present study was approved by the recombinant DNA experiments safety committees of both Okayama University (Approval No. 18089) and International University of Health and Welfare (Approval No. D18001), and the research ethics committees of both Okayama

University (Research No. 1711-018) and the International University of Health and Welfare (Approval No. 14-Io-131).

CYP3A5 genotyping, HLM preparation, and determination of CYP3As content in HLM

Genomic DNA isolation, *CYP3A5*3* genotyping, HLM preparation, and determination of CYP3A4 and CYP3A5 protein contents in each HLM were carried out as described previously (ref. 27). Briefly, genomic DNA was isolated from frozen human liver tissues using DNAzol® (Invitrogen, Carlsbad, CA) according to manufacturer's instruction, and HLMs were prepared using ultracentrifugation methods. The genotyping of *CYP3A5*3* from each human liver was carried out using PCR-restriction fragment length polymorphism method with *Dra*I (Takara, Shiga, Japan) and specific primers (Forward, 5'-CTAACCATAATCTCTTTTAAGAGCTCTTTTGTCTTTAA-3'; Reverse, 5'-ACTTTGATCATTATGTTATGTAATCCATAC-3'). Individual HLMs were used in the correlation analysis, and two pooled HLMs were prepared by mixing equal amounts and concentrations of 12 HLMs genotyped with *CYP3A5*1/*1* or **1/*3* (designated as CYP3A5 expressers) and 27 HLMs genotyped with *CYP3A5*3/*3* (designated as

CYP3A5 non-expressers), respectively.

Measurement of drug-metabolizing activity in rCYP3As and HLM

ASV, DCV, and BCV were dissolved and serially diluted with DMSO to the desired concentrations. Incubation mixtures (300 μL final volume) containing rCYP3A4, rCYP3A5 (50 pmol/mL), or HLMs (1.0 mg/mL), and various concentration of ASV (0–100 μM), DCV (0–100 μM), and BCV (0–150 μM) in 0.1 M potassium phosphate (pH 7.4) were pre-incubated at 37 °C for 10 min. The reaction was initiated by adding NADPH regenerating solution and further incubated at 37 °C before the desired period. For inhibition studies, the CYP3As inhibitor ketoconazole (Wako) was added to the incubation mixtures before pre-incubation and was then incubated with each compound for 60 min. The concentrations of ketoconazole (1 mM) were determined based on referred articles (ref. 27, 28). The final concentration of DMSO was set to be less than 1% in the reaction mixture to minimize its influence on CYP activities. The reaction was terminated by the addition of 1 mL cool acetonitrile/methanol (1:1, v/v) containing an internal standard (IS) RTV (10 ng/mL), followed by aggressive vortexing, and cooling on ice. The mixture was centrifuged at 10,000 x *g* for 5 min at 4 °C. The aliquot of the supernatant was directly injected into a liquid chromatography-tandem mass

spectrometry (LC-MS/MS) system.

LC-MS/MS analysis

The LC-MS/MS system and mobile phase condition were as described previously (ref. 27). The multiple reaction monitoring ion transition was in accordance with studies as follows : *m*/*z* 748→648 for ASV, 764→664 for M3/M7 (the same *m*/*z*) from ASV, 734→634 for M6 from ASV, 557→457 for M9 from ASV, 739→565 for DCV, 755→581 for M3 from DCV, 660→535 for BCV, 646→553 for M1 from BCV (structures are all shown in Figure 1), and 722→296 for RTV (ref 22, 23, 29). Analyst software was used for data acquisition, instrument control, and data analysis. The amount of all the compounds was normalized by an IS. Due to lack of pure metabolite, the peak areas were used to express kinetic parameters for each metabolite formation from the parent compound. To calculate this, the peak area for each sample was divided by the ratio of IS peak area at 0 min to the IS at each time.

Kinetic analysis

Apparent kinetic parameters were determined by the best fitting of one of the following models using GraphPad Prism 5 (GraphPad, San Diego, CA):

Michaelis-Menten equation (eq. 1), allosteric sigmoidal (eq. 2), or substrate inhibition (eq. 3) (ref. 30). V_{max}, K_m, $[S]$, h, S_{50}, and K_i represent maximum enzyme velocity, the Michaelis-Menten constant, substrate concentration, the Hill slope, the substrate concentration needed to achieve a half-maximum enzyme velocity, and the dissociation constant for substrate binding, respectively.

$$v = V_{max}\,[S]/(K_m + [S]) \qquad \text{(eq. 1)}$$

$$v = V_{max}\,[S]^h/(S_{50} + [S]^h) \qquad \text{(eq. 2)}$$

$$v = V_{max}\,[S]/(K_m + [S](1 + [S]/K_i)) \qquad \text{(eq. 3)}$$

V_{max}/K_m value was represented as CL_{int} (intrinsic clearance) (ref. 30). When h exceeded 1.0, CL_{max} (apparent maximal clearance) was calculated by the following formula (eq. 4) (ref. 30).

$$CL_{max} = v/[S] = (V_{max}/S_{50}/h) \times (h - 1)^{1\text{-}1/h} \qquad \text{(eq. 4)}$$

Statistical analysis

Statistical analyses were performed using SPSS version 23.0 (IBM, Chicago, IL). Paired Student's *t* test, Mann-Whitney *U* test, and Pearson's correlation coefficient were used for comparison of two mean groups and for the correlations between two variables. $P < 0.05$ indicated statistical significance.

Results

Detection of ASV, DCV, BCV, and their metabolites

Based on the previous reports (ref. 22, 23, 29), the detection methods for ASV, DCV, and BCV were established with simple modification in the present study. The significant peaks of ASV, DCV, and BCV were detected in the established method (Supplementary figure 1). The linear regression analysis showed that the calibration curve for each compound was well-fitted in the range of 1–600 ng/mL for ASV, 1–800 ng/mL for DCV, and 0.1–50 ng/mL for BCV (Supplementary figure 2). The intra- and inter-day precision and accuracy of the established method were determined by the addition of five concentrations of each compound (Supplementary tables 1–3). The coefficients of variation value (%CV) precision were less than 5%. The mean accuracies calculated as the percentage of the nominal concentration were also less than 5%.

Optimization was performed to detect ASV, DCV, and BCV metabolites based on *m/z* information reported previously (ref. 22, 23, 29). Significant peaks for M3/M7, M6, and M9 from ASV, M3 from DCV, and M1 from BCV were detected (Supplementary Figure 1). Significant correlations between the amounts of the parent compound and the relative peak areas for each metabolite were observed (Figure 1).

Differences in the metabolic activities of ASV, DCV, and BCV between rCYP3A4 and rCYP3A5

The differences in metabolite formations from ASV, DCV, and BCV between rCYP3A4 and rCYP3A5 respectively were investigated. ASV was metabolized by both rCYP3A4 and rCYP3A5 at nearly the same disappearance rate with both enzymes (Supplementary figure 3A). ASV was almost completely metabolized by both rCYP3A4 and rCYP3A5 after 60 min. Regarding ASV metabolites, the allosteric sigmoidal model for M3/M7 and M6 and the Michaelis-Menten model for M9 were fitted (Figures 2A–2C). The detailed kinetic values of each metabolite formation from ASV in rCYP3As are summarized in Tables 1A and 2A. The S_{50} value of M3/M7 formations for rCYP3A5 was lower than that for rCYP3A4, while the S_{50} and K_{m} values of M6 and M9 formations for rCYP3A5 were higher than those for rCYP3A4. The V_{max} value of M6 formation for rCYP3A5 was higher than that for rCYP3A4, while the V_{max} values of M3/M7 and M9 formations for rCYP3A5 were lower than those for rCYP3A4. Considering CL_{int} and CL_{max} values for each formation, M3/M7 formations activity (CL_{max}) by rCYP3A5 was higher than that by rCYP3A4, while M6 and M9 formations activities (CL_{max} for M6 and CL_{int} for M9) by rCYP3A5 were almost half of those by rCYP3A4.

DCV was primarily metabolized by rCYP3A4, with only 20% of DCV remaining after 80 min incubation with rCYP3A4 compared to no significant disappearance after incubation with rCYP3A5 (Supplementary figure 3B). In contrast, BCV was metabolized by both rCYP3A4 and rCYP3A5, although BCV was completely metabolized more quickly by rCYP3A4 (60 min) than by rCYP3A5 (80 min) (Supplementary figure 3C). Regarding DCV and BCV metabolites, substrate inhibition model for M3 from DCV and Michaelis-Menten model for M1 from BCV were fitted (Figures 2D and 2E), respectively. The K_m and V_{max} values of M3 formation from DCV for rCYP3A5 were higher and lower than those for rCYP3A4, respectively. The K_m and V_{max} values of M1 formation from BCV for rCYP3A5 were lower than those for rCYP3A4. Considering the results on CL_{int} values, both DCV and BCV metabolic activities by rCYP3A5 were lower than those by rCYP3A4. In particular, the formation activity of M3 from DCV by rCYP3A5 was almost negligible compared to that by rCYP3A4.

Differences in the metabolic activities of ASV, DCV, and BCV between CYP3A5 expressers and CYP3A5 non-expressers

The metabolic activities of ASV, DCV, and BCV in CYP3A5 expressers were

respectively compared to those in CYP3A5 non-expressers. The results were almost consistent with those obtained from rCYP3As described above. Concerning ASV metabolism in HLMs, the allosteric sigmoidal model for M3/M7 and M6 and the Michaelis-Menten model for M9 were fitted as with those in rCYP3As, respectively (Figures 3A–3C). The detailed kinetic values in HLMs are summarized in Tables 1B and 2B. The S_{50} value of M3/M7 formations for CYP3A5 expressers was comparable to that for CYP3A5 non-expressers, while the S_{50} and K_m values of M6 and M9 formations for CYP3A5 expressers were lower and higher than those for CYP3A5 non-expressers, respectively. The V_{max} values of M3/M7, M6, and M9 formations for CYP3A5 expressers were 1.73, 1.95, and 1.68-times higher than those for CYP3A5 non-expressers, respectively. Considering CL_{int} and CL_{max} values for each formation, M3/M7 and M6 formation activities (CL_{max}) in CYP3A5 expressers were higher than those in CYP3A5 non-expressers, but M9 formation (CL_{int}) in CYP3A5 expressers was comparable to that in CYP3A5 non-expressers. For DCV and BCV metabolism, the substrate inhibition model for M3 from DCV and the Michaelis-Menten model for M1 from BCV were fitted as with those in rCYP3As, respectively (Figures 3D and 3E). The K_m and V_{max} values of M3 formation from DCV in CYP3A5 expressers were higher than and comparable to those in CYP3A5 non-expressers, respectively. The K_m and V_{max}

values of M1 formation from BCV in CYP3A5 expressers were lower than and comparable to those in CYP3A5 non-expressers, respectively. From the data on CL_{int} values, DCV metabolic activity in CYP3A5 expressers was comparable to that in CYP3A5 non-expresser, while BCV metabolism in CYP3A5 expressers was slightly higher than that in CYP3A5 non-expresser.

Correlation between metabolic activities of ASV, DCV, and BCV and the expression level of CYP3As respectively

The correlation between ASV, DCV, and BCV metabolites formations and the expression level of CYP3A proteins in 39 HLMs was determined (Table 3). Regarding ASV metabolism, significant correlations between the formation of all three metabolites, M3/M7, M6, and M9, and CYP3A4 expression level were observed. In addition, it should be noted that the formation of these ASV metabolites were significantly correlated with CYP3A5 expression level. Total of CYP3As (CYP3A4 + CYP3A5) expression level was also significantly correlated with the formation of ASV metabolites. In DCV and BCV metabolism, significant correlations between their metabolite formations and CYP3A4 expression level were observed. The formation of these metabolites was also significantly correlated with total CYP3As expression level,

but there were no correlations between the metabolites formations and CYP3A5 expression level.

Discussion

There has been no detailed information on the contributions of *CYP3A5*3* variant on ASV, DCV, and BCV metabolism, although these drugs are known to be substrates for CYP3As. Here, the detailed relative contributions of CYP3A4 and CYP3A5 to ASV, DCV, and BCV metabolism *in vitro* were elucidated, and the effects of *CYP3A5*3* variant on their metabolism were revealed using rCYP3As and HLMs. Several oxidative metabolite forms of ASV, DCV, and BCV were reported in previous studies (ref. 22, 23, 29). In addition to M3/M7 and M9, it has been reported that M12, which was not the area of focus in the present study, was prominently detected as ASV metabolite in the plasma of male healthy volunteers after ASV administration, and M6 was not observed in their plasma (ref. 22). However, significant peaks of M3/M7, M6, and M9, but not M12, were detected in samples after incubation with rCYP3As as well as HLMs in the present study. These formations of M3/M7, M6, and M9 from ASV were well correlated with the remaining amount of ASV. CYP3As-medicated metabolism for M3/M7, M6, and M9 formations has been proposed, and M6 is known to be further metabolized to M9 followed by M12 formation (ref. 22). However, there is no direct evidence that CYP3As mediate the production of M12 from M9. Summarily, M3/M7, M6, and M9 could be at least considered as the main metabolites of ASV via

CYP3As-mediated metabolism. In DCV and BCV metabolism, M3 from DCV and M1 from BCV were reported to be the main metabolites, respectively (ref. 23, 29). Our results were consistent with these reports. Therefore, M3 and M1 were considered as the main metabolites of DCV and BCV, and these metabolites were further investigated in the present study. Minor contributions by the other CYPs, such as CYP1A2, 2A6, 2B6, 2C8, 2C9, 2C19, 2D6, and 2E1, to ASV metabolism have been reported, but not at significant levels, and no relationship has been shown between these CYPs and the metabolism of DCV and BCV (ref. 22–24). In addition, selective inhibitors of these other CYP enzymes did not inhibit ASV metabolism to a meaningful extent, while the formation of ASV metabolites was strongly inhibited by the presence of ketoconazole. Similarly, substrate probes for CYP1A2, 2C8, 2C9, 2C19, and 2D6 did not affect the area under the concentration-time curve (AUC) of ASV, DCV, and BCV in healthy subjects (ref. 24). Our supplemental results are consistent with these findings: the production of all metabolites of M3/M7, M6, and M9 from ASV, as well as M3 from DCV and M1 from BCV, were strongly inhibited by ketoconazole (Supplementary figure 4). These data indicate that the main contributor to ASV, DCV, and BCV metabolism is CYP3As, and the contribution of other CYP enzymes is negligible.

ASV serum concentration was correlated with liver injury represented as ALT

elevation after ASV administration, and high ASV exposure was observed in subjects with moderate and severe hepatic impairment (ref. 31–33). The discontinuation or reduction in ASV administration improved ALT levels in these patients, indicating that the level of ASV exposure is related to the incidence of AEs. However, the detailed mechanistic factor that could be defined as high-risk patients exhibiting AEs has been unknown. The present study revealed that ASV metabolic activity by CYP3A5 was comparable to or higher than that by CYP3A4. It is well known that the expression level of CYP3A5 protein in CYP3A5 expressers was significant compared to CYP3A4 (ref. 34). Moreover, blood concentration of drugs, such as tacrolimus that has its metabolic activity by CYP3A5 higher than that by CYP3A4 *in vitro*, was high in CYP3A5 non-expressers in clinical settings (ref. 18–20). These indicate that CYP3A5 protein in populations possessing at least one *CYP3A5*1* allele may increase the metabolic ratio of ASV. Indeed, the formation of M3/M7 and M6 in CYP3A5 expressers was higher than that in CYP3A5 non-expressers. The significant correlation between ASV metabolism and CYP3A5 expression level observed in the present study may support this explanation. The reason for the slight difference in results between rCYP3As and HLMs may be because HLMs are more complex than rCYP3As. Each rCYP3A contains only CYP3A4 or CYP3A5, whereas HLMs contain all enzymes in the CYP family. M9 could

be further transformed to other metabolites. It has been reported that CYP3As have a significant role in both hydroxylation and loss of isoquinoline for ASV and its metabolites, while other CYP enzymes may play a weak role in the loss of isoquinoline based on experimental results obtained using inhibitors against each CYP (ref. 22). This could influence the production of each metabolite from another metabolite in the metabolic pathway. This integration of multiple factors, though weak individually, may have the potential to produce the observed differences between the rCYP3As and the HLMs. In any case, CYP3A5 and CYP3A4 are clearly of importance for the production of metabolites from ASV. *CYP3A5*3* variant may therefore affect inter-individual variation in ASV exposure, and this variant may be one of the factors related to high exposure of ASV by decreasing ASV metabolic ratio.

The predominance of CYP3A4-mediated metabolism in DCV has been reported in the drug information provided by the manufacturer as well as in several reports (ref. 23), and it is consistent with the results of the present study. The metabolic activity of DCV by CYP3A5 is far lower than that by CYP3A4. As expected, the importance of CYP3A5 in DCV metabolism was not observed in HLMs. The most significant factor in DCV metabolism is the expression of CYP3A4, and the expression level of CYP3A5 is not related and is not needed to be considered in DCV metabolism.

Therefore, *CYP3A5*3* may not have any clinical effect on DCV metabolism. On the other hand, CL_{max} for BCV in CYP3A5 expressers was higher than that in CYP3A5 non-expresser, while the metabolic activity of BCV by CYP3A5 was lower than that by CYP3A4. However, the difference in CL_{max} for M1 formation between CYP3A5 expressers and CYP3A5 non-expressers was slight, and there was no significant correlation between BCV metabolism and the expression level of CYP3A5. Summarily, the contribution of CYP3A5 expression to BCV metabolism is not completely negligible, and CYP3A5 might possibly be involved in BCV metabolism when CYP3A4 is either in low quantities or functionally impeded, but the contribution of CYP3A5 expression, as well as *CYP3A5*3* variant to BCV metabolism might not be so important compared to ASV metabolism.

CYP3As are involved in numerous drug metabolisms including ASV, DCV, and BCV. CYP3A4 is especially well known to have many drug-drug interactions. Famous CYP3A4 inhibitors such as ketoconazole and ritonavir were reported to strongly increase AUC of ASV, DCV, and BCV, while CYP3A4 inducers such as rifampicin were reported to strongly decrease AUC of ASV and DCV in several reports and drug information from the production company (ref. 35–37). Importantly, there was a clinical report that ASV/DCV administration could decrease the desired dose of tacrolimus in

HCV patients with liver transplantation, and ASV concentration, but not DCV concentration, became lower according to the reduction of tacrolimus dose (ref. 38, 39). This may be because the contribution of CYP3A5 might shift from tacrolimus to ASV according to reduction of tacrolimus dose, while CYP3A5 did not participate in DCV metabolism. In contrast, most of the DCV remains as the unmetabolized form in plasma after administration to healthy volunteers, indicating that CYP3A4 generally has low effects on DCV blood concentration in subjects without co-administration of any other drugs. However, the drug interaction with CYP3A4 should be considered when using drugs that are metabolized by CYP3A4 with DCV. The reports that co-administration of DCV with CYP3A4 inhibitors/inducers significantly changed AUC of DCV, as described above, along with the wide substrate specificity for CYP3A4, may support this explanation. Although there are no clinical reports for BCV, CYP3A5 might not have a strong clinical effect on BCV metabolism based on the present study. In summary, it is essential to consider drug-drug interaction with CYP3A4 substrates when using ASV, DCV, and BCV, but the interaction with drugs that have significant metabolic activity with CYP3A5 should be considered in only ASV. On the other hand, other factors such as drug transporters may involve in ASV, DCV, and BCV disposition. P-glycoprotein and organic anion transporters (OATP) 1B1/1B3 are reported to play a

role in the transport of ASV, DCV, and BCV (ref. 24, 40, 41). These transporters also interact with many other drugs, including statins, anticonvulsants, antivirals, and chemotherapeutics (ref. 42–44). Several substrates for these transporters are also important substrates for CYP3As. To fully understand the pharmacokinetics of ASV, DCV, and BCV, it is necessary to consider the influence of not only CYP3As, but of these transporters as well. Further investigation is needed to assess the utility of the information about these drug transporters for inter-individual variation in ASV/DCV/BCV therapy. In addition to laboratory-based experiments using cultured cells or animals overexpressing/suppressing these drug transporters and using inhibitors/inducers for these transporters, clinical investigation on the utility of combining CYP3As with these transporters is needed.

In conclusion, this study elucidated the detailed relative contributions of CYP3A4 and CYP3A5 to ASV, DCV, and BCV metabolisms. CYP3A5 plays an important role in ASV metabolism, and *CYP3A5*3* variant has a significant effect on ASV metabolism. However, CYP3A4 is the main enzyme for DCV and BCV metabolisms, and CYP3A5 plays a minor role in these metabolisms. The findings of the present study may provide basic information on ASV, DCV, and BCV metabolism and suggest that high ASV exposure may be potentially explained by CYP3A5 expression

level. This study therefore warns against the use of drugs that are substrates for CYP3A5 with co-administration of ASV. In addition, CYP3A4 expression and its substrate levels should be considered when using ASV, DCV, and BCV. The evaluation of CYP3A4 and CYP3A5 expression such as by CYP3A5 genotyping before treatment may provide additional information on precision medicine that could be used to select the best treatment for HCV-infected patients.

Acknowledgements: We acknowledge Drs. Yasuyuki Momose (International University of Health and Welfare, IUHW), Kayoko Maezawa (IUHW), Takeshi Ito (IUHW), and Natsuko Sugiyama (IUHW) for providing useful suggestions. We thank Editage (ww.editage.jp) for English language editing.

This work was supported by the JSPS KAKENHI (Grant-in-Aid for Young Scientists (B), Grant Number: 16K18955).

References

1. Messina JP, Humphreys I, Flaxman A, Brown A, Cooke GS, Pybus OG, et al. Global distribution and prevalence of hepatitis C virus genotypes. Hepatology. 2015;61:77-87.
2. Gower E, Estes C, Blach S, Razavi-Shearer K, Razavi H. Global epidemiology and genotype distribution of the hepatitis C virus infection. J Hepatol. 2014;61:S45-57.
3. Bartenschlager R, Lohmann V, Penin F. The molecular and structural basis of advanced antiviral therapy for hepatitis C virus infection. Nat Rev Microbiol. 2013;11:482-96.
4. Kumada H, Suzuki F, Suzuki Y, Toyota J, Karino Y, Chayama K, et al. Randomized comparison of daclatasvir + asunaprevir versus telaprevir + peginterferon/ribavirin in Japanese hepatitis C virus patients. J Gastroenterol Hepatol. 2016;31:14-22.
5. Pasquinelli C, McPhee F, Eley T, Villegas C, Sandy K, Sheridan P, et al. Single- and multiple-ascending-dose studies of the NS3 protease inhibitor asunaprevir in subjects with or without chronic hepatitis C. Antimicrob Agents Chemother. 2012;56:1838-44.
6. Chayama K, Takahashi S, Toyota J, Karino Y, Ikeda K, Ishikawa H, et al. Dual therapy with the nonstructural protein 5A inhibitor, daclatasvir, and the nonstructural protein 3 protease inhibitor, asunaprevir, in hepatitis C virus genotype

1b-infected null responders. Hepatology. 2012;55:742-8.

7. Kumada H, Suzuki Y, Ikeda K, Toyota J, Karino Y, Chayama K, et al. Daclatasvir plus asunaprevir for chronic HCV genotype 1b infection. Hepatology. 2014;59:2083-91.
8. McPhee F, Hernandez D, Yu F, Ueland J, Monikowski A, Carifa A, et al. Resistance analysis of hepatitis C virus genotype 1 prior treatment null responders receiving daclatasvir and asunaprevir. Hepatology. 2013;58:902-11.
9. McPhee F, Suzuki Y, Toyota J, Karino Y, Chayama K, Kawakami Y, et al. High sustained virologic response to daclatasvir plus asunaprevir in elderly and cirrhotic patients with hepatitis C virus genotype 1b without baseline NS5A polymorphisms. Adv Ther. 2015;32:637-49.
10. Lemm JA, Liu M, Gentles RG, Ding M, Voss S, Pelosi LA, et al. Preclinical characterization of BMS-791325, an allosteric inhibitor of hepatitis C Virus NS5B polymerase. Antimicrob Agents Chemother. 2014;58:3485-95.
11. Pelosi LA, Voss S, Liu M, Gao M, Lemm JA. Effect on hepatitis C virus replication of combinations of direct-acting antivirals, including NS5A inhibitor daclatasvir. Antimicrob Agents Chemother. 2012;56:5230-9.
12. McPhee F, Hernandez D, Zhou N, Ueland J, Yu F, Vellucci V. Pooled analysis of

HCV genotype 1 resistance-associated substitutions in NS5A, NS3 and NS5B pre-and post-treatment with 12 weeks of daclatasvir, asunaprevir and beclabuvir. Antivir Ther. 2018;23:53-66.

13. Poordad F, Sievert W, Mollison L, Bennett M, Tse E, Bräu N, et al. Fixed-dose combination therapy with daclatasvir, asunaprevir, and beclabuvir for noncirrhotic patients with HCV genotype 1 infection. JAMA. 2015;313:1728-35.
14. Daly AK. Significance of the minor cytochrome P450 3A isoforms. Clin Pharmacokinet. 2006;45:13-31.
15. Westlind A, Malmebo S, Johansson I, Otter C, Andersson TB, Ingelman-Sundberg M, et al. Cloning and tissue distribution of a novel human cytochrome p450 of the CYP3A subfamily, CYP3A43. Biochem Biophys Res Commun. 2001;281:1349-55.
16. Williams JA, Ring BJ, Cantrell VE, Jones DR, Eckstein J, Ruterbories K, et al. Comparative metabolic capabilities of CYP3A4, CYP3A5, and CYP3A7. Drug Metab Dispos. 2002;30:883-91.
17. Niwa T, Murayama N, Emoto C, Yamazaki H. Comparison of kinetic parameters for drug oxidation rates and substrate inhibition potential mediated by cytochrome P450 3A4 and 3A5. Curr Drug Metab. 2008;9:20-33.
18. Dai Y, Hebert MF, Isoherranen N, Davis CL, Marsh C, Shen DD, et al. Effect of

CYP3A5 polymorphism on tacrolimus metabolic clearance in vitro. Drug Metab Dispos. 2006;34:836-47.

19. Jacobson PA, Oetting WS, Brearley AM, Leduc R, Guan W, Schladt D, et al. Novel polymorphisms associated with tacrolimus trough concentrations: results from a multicenter kidney transplant consortium. Transplantation. 2011;91:300-8.
20. Niioka T, Kagaya H, Saito M, Inoue T, Numakura K, Habuchi T, et al. Capability of utilizing CYP3A5 polymorphisms to predict therapeutic dosage of tacrolimus at early stage post-renal transplantation. Int J Mol Sci. 2015;16:1840-54.
21. Hsu MH, Savas U, Johnson EF. The X-Ray Crystal Structure of the Human Mono-Oxygenase Cytochrome P450 3A5-Ritonavir Complex Reveals Active Site Differences between P450s 3A4 and 3A5. Mol Pharmacol. 2018;93:14-24.
22. Gong J, Eley T, He B, Arora V, Philip T, Jiang H, et al. Characterization of ADME properties of [^{14}C] asunaprevir (BMS-650032) in humans. Xenobiotica. 2016;46:52-64.
23. Li W, Zhao W, Liu X, Huang X, Lopez OD, Leet JE. et al. Biotransformation of daclatasvir in vitro and in nonclinical species: formation of the main metabolite by pyrrolidine δ-oxidation and rearrangement. Drug Metab Dispos. 2016;44:809-20.
24. Garimella T, Tao X, Sims K, Chang YT, Rana J, Myers E, et al. Effects of a

Fixed-Dose Co-Formulation of Daclatasvir, Asunaprevir, and beclabuvir on the pharmacokinetics of a cocktail of cytochrome P450 and drug transporter substrates in healthy subjects. Drugs R D. 2018;18:55-65.

25. Kuehl P, Zhang J, Lin Y, Lamba J, Assem M, Schuetz J, et al. Sequence diversity in CYP3A promoters and characterization of the genetic basis of polymorphic CYP3A5 expression. Nat Genet. 2001;27:383-91.
26. Toyota J, Karino Y, Suzuki F, Ikeda F, Ido A, Tanaka K, et al. Daclatasvir/asunaprevir/beclabuvir fixed-dose combination in Japanese patients with HCV genotype 1 infection. J Gastroenterol. 2017;52:385-95.
27. San SN, Matsumoto J, Saito Y, Koike M, Sakaue H, Kato Y, et al. Minor contribution of CYP3A5 to the metabolism of hepatitis C protease inhibitor paritaprevir in vitro. Xenobiotica. 2019;49:935-44.
28. Walsky RL, Obach RS, Hyland R, Kang P, Zhou S, West M, et al. Selective mechanism-based inactivation of CYP3A4 by CYP3cide (PF-04981517) and its utility as an in vitro tool for delineating the relative roles of CYP3A4 versus CYP3A5 in the metabolism of drugs. Drug Metab Dispos. 2012;40:686–97.
29. Yuan L, Jiang H, Zheng N, Xia YQ, Ouyang Z, Zeng J, et al. A validated LC-MS/MS method for the simultaneous determination of BMS-791325, a hepatitis

C virus NS5B RNA polymerase inhibitor, and its metabolite in plasma. J Chromatogr B Analyt Technol Biomed Life Sci. 2014;15:973C:1-8.

30. Houston JB, Kenworthy KE. In vitro-in vivo scaling of CYP kinetic data not consistent with the classical Michaelis-Menten model. Drug Metab Dispos. 2000;28:246-54.
31. Uchida Y, Naiki K, Kouyama JI, Sugawara K, Nakao M, Motoya D, et al. Serum asunaprevir concentrations showing correlation with the extent of liver fibrosis as a factor inducing liver injuries in patients with genotype-1b hepatitis C virus receiving daclatasvir plus asunaprevir therapy. PLoS One. 2018;13:e0205600.
32. Akuta N, Sezaki H, Suzuki F, Kawamura Y, Hosaka T, Kobayashi M, et al. Relationships between serum asunaprevir concentration and alanine aminotransferase elevation during daclatasvir plus asunaprevir for chronic HCV genotype 1b infection. J Med Virol. 2016;88:506-11.
33. Eley T, He B, Chang I, Colston E, Child M, Bedford W, et al. The effect of hepatic impairment on the pharmacokinetics of asunaprevir, an HCV NS3 protease inhibitor. Antivir Ther. 2015;20:29–37.
34. Lin YS, Dowling AL, Quigley SD, Farin FM, Zhang J, Lamba J, et al. Co-regulation of CYP3A4 and CYP3A5 and contribution to hepatic and intestinal

midazolam metabolism. Mol Pharmacol. 2002;62:162-72.

35. Poole RM. Daclatasvir + asunaprevir: first global approval. Drugs. 2014;74:1559-71.

36. Mosure KW, Knipe JO, Browning M, Arora V, Shu YZ, Phillip T, et al. Preclinical pharmacokinetics and in vitro metabolism of asunaprevir (BMS-650032), a potent hepatitis C virus NS3 protease inhibitor. J Pharm Sci. 2015;104:2813-23.

37. Dogra A, Bhatt S, Magotra A, Sharma A, Kotwal P, Gour A, et al. Intervention of curcumin on oral pharmacokinetics of daclatasvir in rat: A possible risk for long-term use. Phytother Res. 2018;32:1967-74.

38. Harada N, Yoshizumi T, Ikegami T, Itoh S, Furusho N, Kato M, et al. Serum asunaprevir and daclatasvir concentrations and outcomes in patients with recurrent hepatitis C who have undergone living donor liver transplantation. Anticancer Res. 2018;38:5513-20.

39. Bifano M, Adamczyk R, Hwang C, Kandoussi H, Marion A, Bertz RJ. An open-label investigation into drug–drug interactions between multiple doses of daclatasvir and single-dose cyclosporine or tacrolimus in healthy subjects. Clin Drug Investig. 2015;35:281-9.

40. Furihata T, Matsumoto S, Fu Z, Tsubota A, Sun Y, Matsumoto S, et al. Different

interaction profiles of direct-acting anti-hepatitis C virus agents with human organic anion transporting polypeptides. Antimicrob Agents Chemother. 2014;58:4555-64.

41. Eley T, Han YH, Huang SP, He B, Li W, Bedford W, et al. Organic anion transporting polypeptide-mediated transport of, and inhibition by, asunaprevir, an inhibitor of hepatitis C virus NS3 protease. Clin Pharmacol Ther. 2015;97:159-66.
42. Shitara Y, Maeda K, Ikejiri K, Yoshida K, Horie T, Sugiyama Y. Clinical significance of organic anion transporting polypeptides (OATPs) in drug disposition: their roles in hepatic clearance and intestinal absorption. Biopharm Drug Dispos. 2013;34:45-78.
43. Nakanishi T, Tamai I. Interaction of Drug or Food with Drug Transporters in Intestine and Liver. Curr Drug Metab. 2015;16:753-64.
44. Saravanakumar A, Sadighi A, Ryu R, Akhlaghi F. Physicochemical Properties, Biotransformation, and Transport Pathways of Established and Newly Approved Medications: A Systematic Review of the Top 200 Most Prescribed Drugs vs. the FDA-Approved Drugs Between 2005 and 2016. Clin Pharmacokinet. In press 2019.

Titles and legends to figures

Figure 1. The chemical structures of ASV, DCV, BCV, and their metabolites (M3/M7, M6, and M9 for ASV; M3 for DCV; M1 for BCV), and the correlation between the percentage of parent compound residues and the relative peak area of their metabolites (A, B, and C are for ASV, DCV, and BCV, respectively). Putative main metabolic enzymes and their reaction patterns are also represented. The chemical structures were provided by the pharmaceutical company Bristol-Myers Squibb (New York City, NY). For metabolite formations, each parent compound was incubated with 39 HLMs for 20 min at 37 °C. The values were expressed as percentages calculated from 0 min of incubation and normalized by IS.

Figure 2. The difference in M3/M7 (A), M6 (B), M9 (C), M3 (D), and M1 (E) formation activities between rCYP3A4 and rCYP3A5. Open and closed circles represent each formation for rCYP3A4 and rCYP3A5, respectively. Various concentrations of each parent compound were incubated with either rCYP3A4 or CYP3A5 at 37 °C for 20 min. The data are represented as the peak areas for each metabolite normalized by IS. The substrate concentration-velocity and the corresponding Eadie–Hofstee plot are also shown. Each data point represents the mean of triplicate incubations, and error bars represent the SD.

Figure 3. The difference in M3/M7 (A), M6 (B), M9 (C), M3 (D), and M1 (E) formation activities between CYP3A5 expressers and CYP3A5 non-expressers. Closed and open circles represent each formation for CYP3A5 expressers and CYP3A5 non-expressers, respectively. Various concentrations of each parent compound were incubated with HLMs at 37 °C for 20 min. The data are represented as the peak areas for each metabolite normalized by IS. The substrate concentration-velocity and the corresponding Eadie–Hofstee plot are also shown. Each data point represents the mean of triplicate incubations, and error bars represent the SD.

A

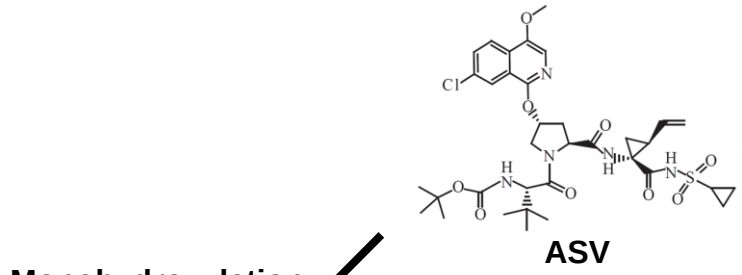

ASV

Monohydroxylation

CYP3A

CYP3A

O-demethylation

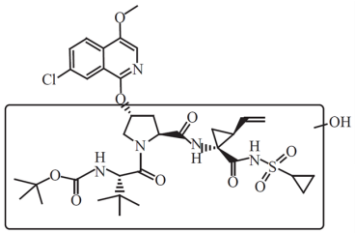

ASV M3/M7

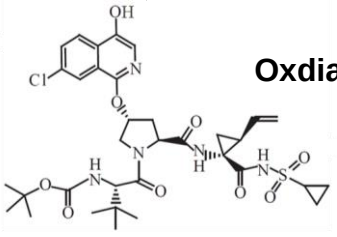

ASV M6

Oxdiation of isoquinoline

CYP3A

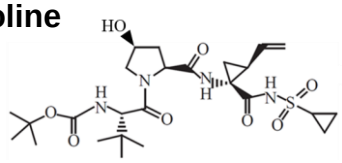

ASV M9

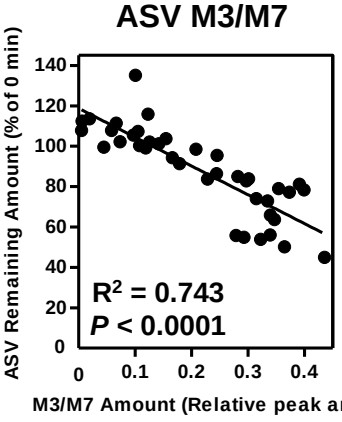

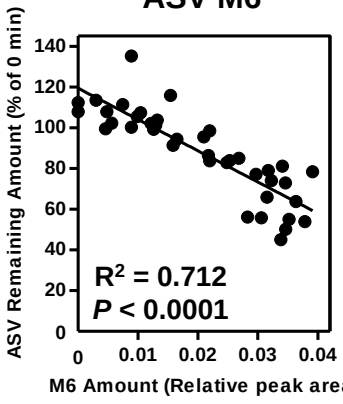

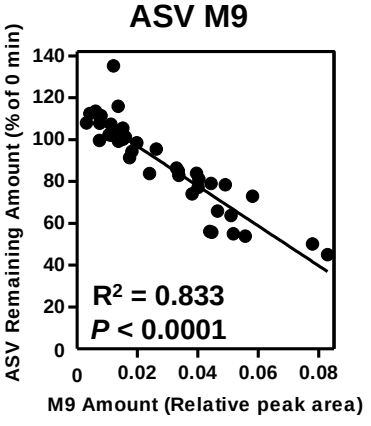

B

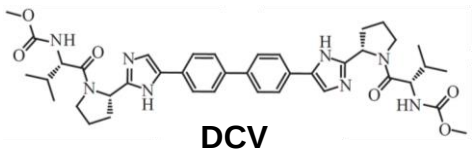

DCV

N-dealkylation

CYP3A

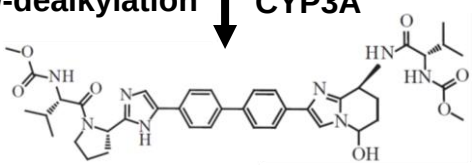

DCV M3

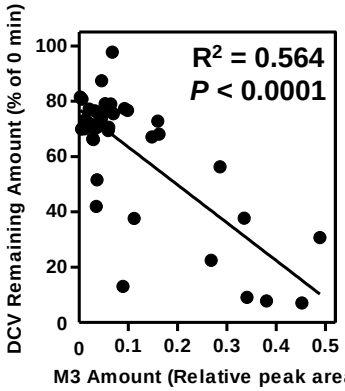

C

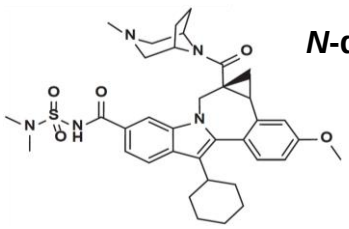

BCV

N-demethylation

CYP3A

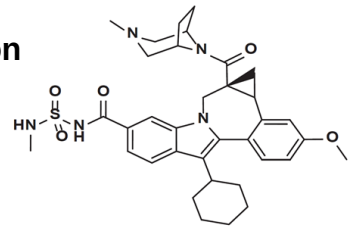

BCV M1

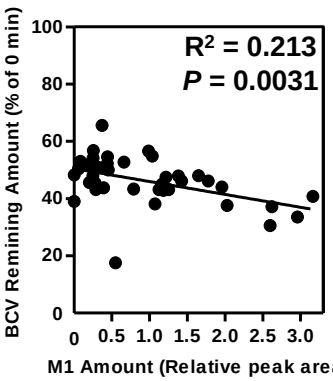

Figure 2

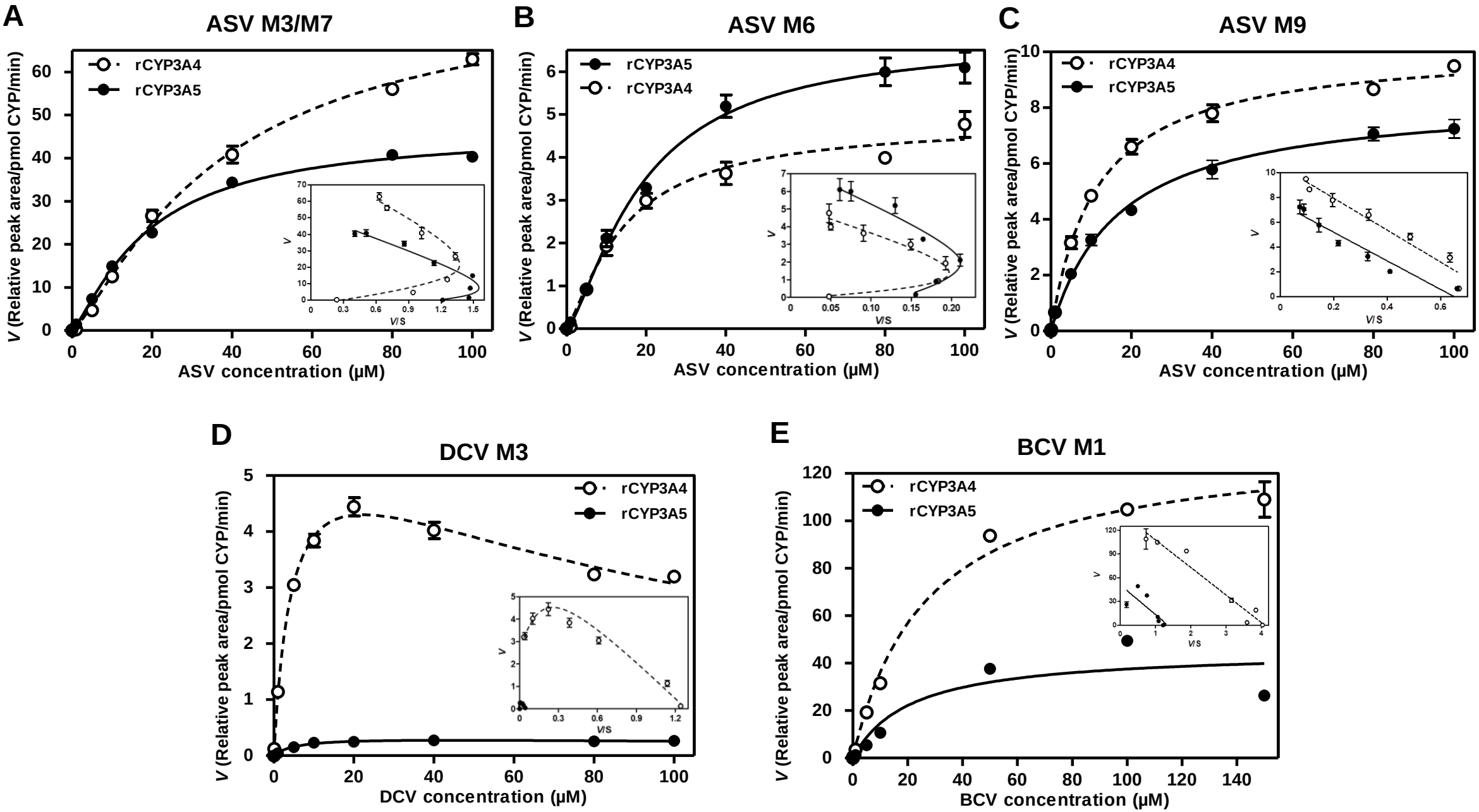
A
ASV M3/M7
rCYP3A4
rCYP3A5
V (Relative peak area/pmol CYP/min)
ASV concentration (μM)
V/S
B
ASV M6
rCYP3A5
rCYP3A4
V (Relative peak area/pmol CYP/min)
ASV concentration (μM)
V/S
C
ASV M9
rCYP3A4
rCYP3A5
V (Relative peak area/pmol CYP/min)
ASV concentration (μM)
V/S
D
DCV M3
rCYP3A4
rCYP3A5
V (Relative peak area/pmol CYP/min)
DCV concentration (μM)
V/S
E
BCV M1
rCYP3A4
rCYP3A5
V (Relative peak area/pmol CYP/min)
BCV concentration (μM)
V/S

Figure 3

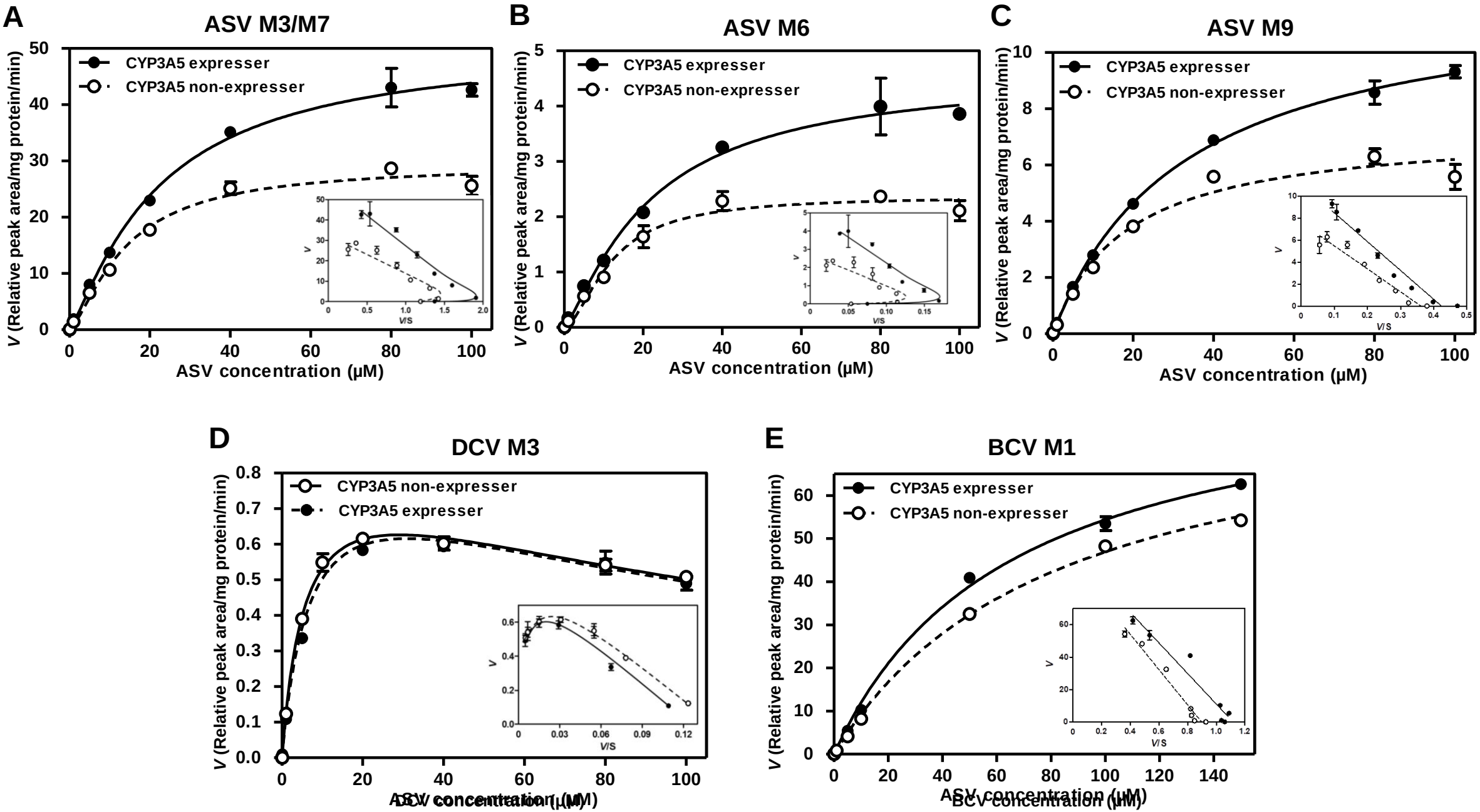
A
ASV M3/M7
CYP3A5 expresser
CYP3A5 non-expresser
V (Relative peak area/mg protein/min)
ASV concentration (μM)
V/S
B
ASV M6
CYP3A5 expresser
CYP3A5 non-expresser
V (Relative peak area/mg protein/min)
ASV concentration (μM)
V/S
C
ASV M9
CYP3A5 expresser
CYP3A5 non-expresser
V (Relative peak area/mg protein/min)
ASV concentration (μM)
V/S
D
DCV M3
CYP3A5 non-expresser
CYP3A5 expresser
V (Relative peak area/mg protein/min)
DCV concentration (μM)
V/S
E
BCV M1
CYP3A5 expresser
CYP3A5 non-expresser
V (Relative peak area/mg protein/min)
BCV concentration (μM)
V/S

Table 1. Kinetic parameters for ASV, DCV, and BCV metabolite formations by rCYP3As (A) and *CYP3A5*3*-genotyped HLMs (B).

A. Recombinant CYP3As

Metabolite		CYP3A4				CYP3A5			
		K_m or S_{50}	V_{max}	Hill slope	Type	K_m or S_{50}	V_{max}	Hill slope	Type
ASV	M3/M7	94.41 (S_{50})	79.30	1.259	Sigmoid	40.66 (S_{50})	46.45	1.259	Sigmoid
	M6	29.11 (S_{50})	4.81	1.260	Sigmoid	59.06 (S_{50})	6.80	1.385	Sigmoid
	M9	11.31 (K_m)	10.21	-	Michaelis	16.91 (K_m)	8.42	-	Michaelis
DCV	M3	4.66 (K_m)	6.11	-	Inhibition	5.78 (K_m)	0.34	-	Inhibition
BCV	M1	26.83 (K_m)	133.00	-	Michaelis	21.05 (K_m)	45.44	-	Michaelis

B. HLMs

Metabolite		Non-Expresser				Expresser			
		K_m or S_{50}	V_{max}	Hill slope	Type	K_m or S_{50}	V_{max}	Hill slope	Type
ASV	M3/M7	38.94 (S_{50})	29.44	1.392	Sigmoid	41.62 (S_{50})	51.03	1.203	Sigmoid
	M6	63.67 (S_{50})	2.37	1.680	Sigmoid	46.28 (S_{50})	4.62	1.244	Sigmoid
	M9	18.17 (K_m)	7.33	-	Michaelis	32.69 (K_m)	12.28	-	Michaelis
DCV	M3	5.83 (K_m)	0.88	-	Inhibition	7.15 (K_m)	0.90	-	Inhibition
BCV	M1	82.21 (K_m)	85.50	-	Michaelis	65.34 (K_m)	89.92	-	Michaelis

K_m or S_{50}, μM; V_{max}, Relative peak area/pmol CYP/min for recombinant CYP3As or relative peak area/pmol protein/min for HLMs

Table 2. Differences in CL_{int} and CL_{max} values for ASV, DCV, and BCV metabolite formations between rCYP3A4 and rCYP3A5 (A) or CYP3A5 expressers and CYP3A5 non-expressers (B).

A. Recombinant CYP3As

Metabolite		CL_{int} or CL_{max}		3A5/3A4 ratio
		CYP3A4	CYP3A5	
ASV	M3/M7	0.505 (CL_{max})	0.687 (CL_{max})	1.360
M6		0.099 (CL_{max})	0.063 (CL_{max})	0.641
	M9	0.903 (CL_{int})	0.498 (CL_{int})	0.551
DCV	M3	1.308 (CL_{int})	0.059 (CL_{int})	0.045
BCV	M1	4.957 (CL_{int})	2.159 (CL_{int})	0.435

B. HLMs

Metabolite		CL_{int} or CL_{max}		Expresser/Non-expresser ratio
		Non-expresser	Expresser	
ASV	M3/M7	0.417 (CL_{max})	0.779 (CL_{max})	1.867
M6		0.019 (CL_{max})	0.061 (CL_{max})	3.207
	M9	0.403 (CL_{int})	0.376 (CL_{int})	0.932
DCV	M3	0.151 (CL_{int})	0.126 (CL_{int})	0.837
BCV	M1	1.040 (CL_{int})	1.376 (CL_{int})	1.323

Table 3. Correlation between CYP3A expression profiles and ASV, DCV, and BCV metabolisms.

Metabolite		CYP3A4	CYP3A5	CYP3As (3A4 +3A5)
ASV	M3/M7	***P* < 0.001** (*r* = 0.525)	***P* < 0.05** (*r* = 0.342)	***P* < 0.001** (*r* = 0.621)
	M6	***P* < 0.001** (*r* = 0.624)	***P* < 0.05** (*r* = 0.337)	***P* < 0.001** (*r* = 0.683)
	M9	***P* < 0.001** (*r* = 0.552)	***P* < 0.05** (*r* = 0.328)	***P* < 0.001** (*r* = 0.622)
DCV	M3	***P* < 0.001** (*r* = 0.667)	*P* = 0.878 (*r* = -0.025)	***P* < 0.001** (*r* = 0.525)
BCV	M1	***P* < 0.001** (*r* = 0.681)	*P* = 0.372 (*r* = 0.147)	***P* < 0.001** (*r* = 0.633)

r represents Pearson's correlation coefficient.